DE GRUYTER OPEN

Vol. 11, Issue 2/2015, 95-102 DOI: 10.1515/cee-2015-0012

ASSESSMENT OF STEEL REINFORCEMENT CORROSION STATE BY PARAMETERS OF POTENTIODYNAMIC DIAGRAMS

Ľudovít KRAJČI[1], Ján JERGA[2,*]

[1] Institute of Construction and Architecture, Dúbravská cesta 9, 845 03 Bratislava.
[2] Langsfeldova 19, 811 04 Bratislava.
[*] corresponding author: usarjrg@savba.sk.

Abstract

The environment of the steel reinforcement has a significant impact on the durability and service life of a concrete structure. It is not only the presence of aggressive substances from the environment, but also the own composition of concrete mixture. The use of new types of cements, additives and admixtures must be preceded by verification, if they themselves shall not initiate the corrosion. There is a need for closer physical expression of the parameters of the potentiodynamic diagrams allowing reliable assessment of the influence of the surrounding environment on electrochemical behaviour of reinforcement. The analysis of zero retardation limits of potentiodynamic curves is presented.

Keywords:

Corrosion;
Steel;
Cement Composites;
Potentiodynamic diagrams;
Limit and interval of zero retardation.

1. Introduction

The harmlessness of environment is at the center of our daily concerns. We are disquiet about the poor quality of the air we breathe and avoid places with high risk of bacterial infection. As equally important we consider the social environment with different risks and hazards. The choice of Lot to pitch his tents near Sodom [1] has proved to be a result of a wrong assessment of a community environment with fatal consequences. In general, the seriousness of the environmental question is even more emphasized by its sustained and repeated character.

With regard to the severity of consequences it is understandable the great attention paid to the environment of structures often susceptible to corrosion. Though generally accepted, that cement composites due to their alkaline environment constitute favourable conditions for the corrosion protection of steel, there is a need for caution when structures are exposed to aggressive agents from air pollution, contaminated groundwater or de-icing salts. Extremely important is the modification of properties by use of additives and admixtures to concrete and especially by development of new types of cementitious materials. It is of utmost importance to evaluate the influence of environment on steel corrosion.

The exposure tests at identical conditions, though most reliable, are unrealistic with respect to their duration (tens of years). Widely used for the characterization of the steel reinforcement corrosion in the particular environment is the method based on the evaluation of *potentiodynamic polarization diagrams* [2]. In principle, it is an accelerated corrosion process of steel immersed in a surrounding environment – at RC mostly alkaline. The dissolution of steel initiates its corrosion as an electrochemical process. An atom of iron at surface of steel in contact with a liquid phase transformed into positively charged iron ion is absorbed into the electrolyte, while the negatively charged electron remains on the steel (anodic reaction). To satisfy the electrical equilibrium the electron will pass out at other place of iron surface, consumed at the reaction of oxygen with liquid phase, giving rise to the origin of hydroxyl ions (cathodic reaction). Depending on the potential applied and pH value of the environment the hydrogen gas can be formed, as seen in Pourbaix diagram [3] (both for SHE and SCE). The ongoing processes could be significantly affected by the presence of various substances.

The correlation between resulting electrical current and the potential could be a tool for characterization of the corrosion rate. The Slovak standard [4] describes a testing method at which

the *polarization diagram* is constructed at artificially applied potential difference between steel (or steel in concrete) and reference saturated calomel electrode (SCE) as standard in an aqueous solution, when measuring the *current density* in the electrical circuit closed through relevant solution, and platinum auxiliary electrode. Thus, three-electrode measuring system is established (working electrode – measured steel, reference electrode – SCE; auxiliary electrode - platinum). The electrochemical potential is defined in [3] as a measure of the ease of electron charge transfer between the steel and the cement paste pore solution; it is a property of the steel/concrete interface and not of the steel itself. It could be measured either the change of the *current density* in the dependence on the change of the *potential (potentiodynamic method, voltammetry)*, or the change of the potential depending on the change of the density of the current passing through the sample (*galvanodynamic method, amperometry*). The polarization diagram comprises of an anodic and a cathodic part. Due to the dissolution of steel the attention is paid more often to the *anodic curve*.

The pH value of the real pore solution is between 13.0 and 13.5 for intact concrete, hence the anodic half-cell reaction could be described (considering the Pourbaix diagram [3]) as:

$$\mathrm{Fe} \rightarrow \mathrm{Fe}^{2+} + 2\mathrm{e}^{-}, \tag{1}$$

$$2\mathrm{Fe}^{2+} + 4\mathrm{OH}^{-} \rightarrow 2\mathrm{Fe(OH)}_2, \tag{2}$$

and the origin of iron oxides Fe_3O_4 and Fe_2O_3 (or hydroxides of these compounds) could be expected. They will develop a protective – passive layer on the steel surface, which will inhibit the corrosion by the diffusion barrier.

The dependence of current density on the change of potential is schematically depicted in Fig. 1 [5]. With the progress of anodic polarization (from E_{eq} – equilibrium potential) the increase of current will be registered in the initial part of the diagram (AB), resulting contemporary in the creation of passive film. It is referred as an area corresponding to active region (up to *critical primary passivation potential* E_{pp} [6] and *critical current density* i_{crit}). After *transition region* (BC), characterized by the decrease of current density by increasing the potential, the impeded access of media to reinforcement will be reflected in a nearly constant magnitude of current density (i_p) at increasing potential, called as the *passive region* (CD) [7]. The most negative potential in this state is called the *Flade potential* E_F [5, 6]. The *passive current density* i_p is a measure of the protectiveness of the created film and decreases with the increase of the pH value. The subsequent increase of current could be caused by localized breakdown of the film by e.g. chloride ions, eventually leading to formation of pits. This occurs at the *critical breakdown or pitting potential* E_b (D). If the breakdown of the film by aggressive anions does not occur, the increase of anodic current will occur along the curve FG – corresponding to oxidation of metal at formation of soluble ions (*transpassive dissolution*) and eventually to release of oxygen in given system. The onset of the *secondary passivity* may be observed in some cases.

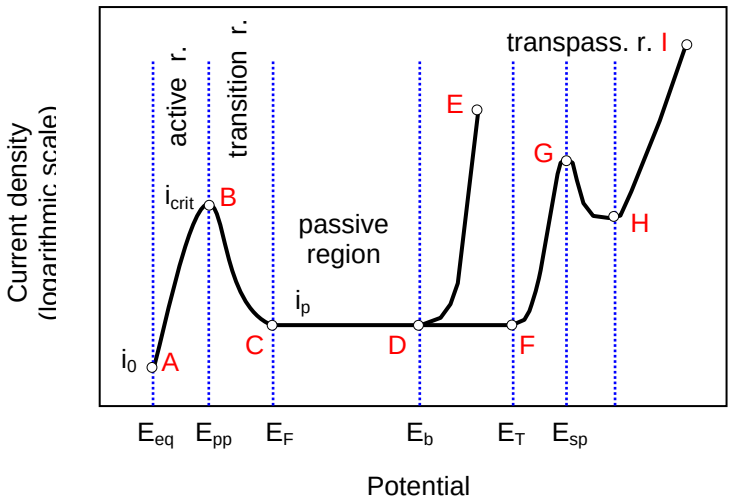

Fig. 1: Potentiodynamic curve of steel [5].

The course of the potentiodynamic diagram is not always regular as visible in Fig. 2 [8], hence the shape alone may not be sufficient to identify the ongoing processes and the quality of the environment. It is especially in cases where it is not possible the mutual comparison of results, as it is e.g. at artificially designed experiments with continuously changing parameters. Therefore numerical models based on real parameters are required for the reliable characterization and assessment.

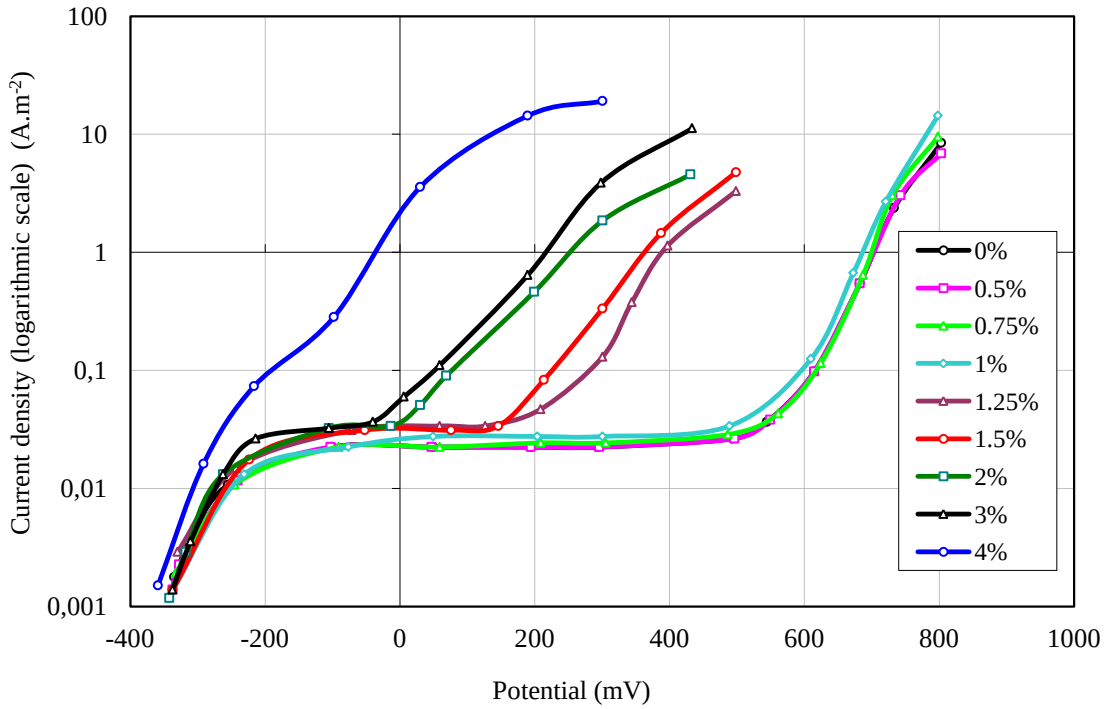

Fig. 2: Potentiodynamic curves of steel reinforcement in extracts of mortar samples at the polarization rate 30 mV.min^{-1} (40 cycles) with different content of calcium chloride in mortar by % of cement weight [8].

2. Numerical models of potentiodynamic diagrams

The dissolution of metals by transfer of current is quantitatively described by *Faraday's laws of electrolysis* [9]. The amount of dissolved metal *m* (g) at an electrode is expressed as:

$$m = \left(\frac{Q}{F}\right)\left(\frac{M}{z}\right), \tag{3}$$

where *Q* is the total electric charge (C) passed through the substance, *F* the Faraday constant equal to 96 485 C.mol^{-1}, *M* is the molar mass of the metal (g.mol^{-1}) and *z* the valency number of ions of the substance (electrons transferred per ion).

At constant current *I* (A), $Q = I.t$, (*t* is the transit time):

$$m = \left(\frac{It}{F}\right)\left(\frac{M}{z}\right). \tag{4}$$

After immersion of the metal electrode into a solution of its own ions an *equilibrium potential* E_{eq} will be established. It is expressed by the *Nernst equation*:

$$E_{eq} = E^{\circ} - \frac{RT}{zF} ln \frac{a_{red}}{a_{ox}}, \tag{5}$$

where E^{o} is the standard half-cell (reduction or oxidation) potential, *R* is the universal gas constant (8.314 JK^{-1}mol^{-1}), *T* the absolute temperature (K), a_{red} and a_{ox} the reductant and oxidant activities (frequently replaced by concentrations).

The standard half-cell potential characterizes the nobility of the metal. Positive potential corresponds to noble metals, resistant to corrosion (for gold E^o = 1.56 V), in the direction to negative potentials there occur base metals (for iron E^o =-0.44 V). Because the potential of an electrode could not be measured separately, there is measured the potential difference to a standard electrode with defined zero potential (usually Standard hydrogen electrode – E_{SHE}=0 V), mutually connected with a salt bridge (saturated solution of potassium chloride).

The dependence of the electrode current *I* on the potential, if both a cathodic and an anodic reaction occur on the same electrode is described by the *Butler-Volmer equation*:

$$i = i_0.\left\{exp\left[\frac{\alpha_a zF}{RT}\left(E - E_{eq}\right)\right] - exp\left[-\frac{\alpha_c zF}{RT}\left(E - E_{eq}\right)\right]\right\}, \quad (6)$$

where (in addition to previous) *i* is the electrode current density defined as the ratio of the electrode current *I* (A) and the electrode active surface area (m^2), i_0 the *exchange current density* ($A.m^{-2}$), defined as the current in the absence of net electrolysis and at zero overpotential, *E* the electrode potential (V), E_{eq} the equilbrium potential (V) and α_a (α_c) the anodic (cathodic) charge transfer coefficient (dimensionless). The difference $E - E_{eq}$ is called as *activation overpotential* and is denoted as η. Eq. (6) represents a total current – sum of anodic and cathodic currents. The course of respective polarization diagrams is in Fig. 3 [9]. At equilibrium potential E_{eq} the exchange current density corresponds both to anodic and cathodic polarization curve. Change of the equilibrium will result in a new state. If the overpotential $\eta > 0$ the anodic reaction will predominate and the metal will dissolve. The extent of the potential change (V) caused by the net current at the electrodes is termed *polarization* [10]. The polarization could be caused by *activation, concentration* (differences of concentration of the reactive substance at the surface of the electrode and in the solution) or *Ohmic potential drop,* due to electrical resistance of the electrolyte between electrodes. At the anodic polarization at steel corrosion in concrete structures the anodic polarization is the only cause [11].

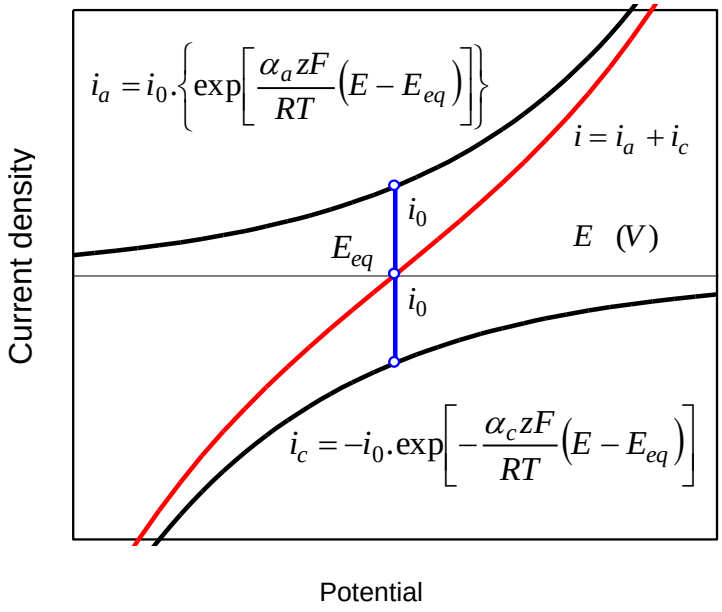

Fig. 3: The course of polarization curve of steel in the vicinity of equilibrium potential E_{eq} [9].

In the low overpotential region ($E \approx E_{eq}$), called as *polarization resistance* (formal similarity with the Ohm's law), the Butler-Volmer equation for an anodic branch simplifies to a linear form:

$$i_a = i_{a0}\frac{\alpha zF}{RT}\left(E - E_{eq}\right) = i_{a0}\frac{2.303\eta_a}{\beta_a}, \quad (7)$$

and in the high overpotential region, for an anodic reaction ($E >> E_{eq}$), to the *Tafel equation*:

$$\eta_a = E - E_{eq} = \beta_a log \frac{i_a}{i_{a0}}, \quad (8)$$

where index *a* means anode and β_a is the Tafel slope (V), usually measured experimentally or defined as:

$$\beta_a = \frac{2.303RT}{\alpha zF}. \quad (9)$$

The numerical value 2.303 represents the transfer between the natural and common logarithms. The inverse relation of Eq. (8) is the Butler-Volmer relation for the anodic reaction (Eq. 6 is written for both anodic and cathodic reactions):

$$i_a = i_{a0} e^{\frac{2.303\eta_a}{\beta_a}}. \quad (10)$$

It should be emphasized [12], that the currents measured during polarization (influencing the shape of the polarization curve) are the function of the transfer of electrons at the electrode/electrolyte interface (charge transfer controlled current), so as of the movement of reactants or products at distances close to the electrode (mass transport controlled current). Only the pure charge transfer controlled current could be accepted as a base for true Tafel data.

After the discontinuity of the polarization curve between the active and passive region (Flade potential [13]) the charge transfer is controlled by the diffusion barrier of the passive layer. Based on their structure, the films are divided into two groups [5] – discontinuous and continuous. The first one, formed at potentials close to the equilibrium potential, is porous and has a low protectiveness. The continuous film has a high resistivity and a maximum thickness of approximately 10^{-3}mm. Various models have been created to explain the growth, structure and operation of oxide films. They could be subdivided into two categories – models explaining the electric properties of passive films by their composition and structure and those emphasising the transport of mass and charge in the film [5]. To the first group belong the *semiconductor models* [14] (metallic conductivity of the inner Fe_3O_4 layer of the film and semiconductor or insulator behaviour of the outer Fe_2O_3 layer) and *chemi-conductor models* [15] (single phase insulator influenced by oxidative and reductive changes of the valence state). The methods of the second group differ by the consideration of the electric field strength in the oxide film, what is reflected in the mathematical treatment of the transport. The *high-field model* [16] supposes, that the driving force for the transport of charge carriers in the film is a high electric field. In the *Mott-Cabrera model* [17], it is assumed, that the film growth is due to the transport of metal cations across the oxide film and the following reaction with the electrolyte. The transport of the moving species at the *Vetter-Kirchheim model* [18] is expected either by a cation vacancy, an anion vacancy or an interstitial cation mechanism. *Model for the impedance response of passive films on transition metals and alloys* [19] assumes both the charge transfer reactions at the interfaces and the transport of ionic species in the film.

One of the most recognized is the *Point Defect Model* (PDM) [20]. It is based on the assumption, that the oxide film contains point defects – cation and anion vacancies, electrons and electron holes. The transport of charge carriers is mutually independent and the transport of ions is described by the Nernst-Planck equation. Further modifications of PDM relate to the possibility of metal cations to contribute not only to the metal dissolution, but also to the film growth, so as the inclusion of the adsorption of water molecules at the film/solution interface in the model. The *Mixed Conduction Model* (MCM), presented in [5, 21], is based on the features of PDM. It is assumed, that the electric field strength in the film is homogeneous and independent on potential, while the film thickness is proportional to the applied potential. The high-field approximation is used for the transport of ionic species at room temperature. The transport equation could be written as:

$$J_o = \frac{D_o}{2a} exp \frac{zFaE}{RT} \left\{ c_o(0) exp\left[-\frac{L}{a}\right] - c_o(L) \right\}, \quad (11)$$

where (in addition to previous) J_o is the flux of oxygen vacancies in the film (mol.cm^{-2}.s^{-1}), D_o the diffusion coefficient of oxygen vacancies (cm^2.s^{-1}), *a* the atomic jump distance (cm), *E* the electric field strength (V.cm^{-1}), c_o (mol.cm^{-3}) the concentration profile of oxygen vacancies in

the film at the metal/film interface and *L* the oxide film thickness (zero value corresponds to film/solution interface). The local electric conductivity is linearly dependent on the local ionic defect concentration. The scheme of processes during the *transpassive dissolution* is presented in [22, 23].

3. Parameters of potentiodynamic diagrams from experimental results

The models, referred to in the previous, based on physical parameters, provide the possibility to express realistic the processes associated with corrosion of steel reinforcement in cement composites. It is therefore essential to focus on description of changes by use of first and second order derivatives of current density according to the potential. An example of potentiodynamic diagrams of steel reinforcement in extracts of mortar samples at the polarization rate 30 mV.min^{-1} (40 cycles) with different content of calcium chloride in mortar by % of cement weight [8] is presented in Fig. 2. The mortar was composed from cement and silica sand in proportion 1 : 3, the w/c was 0.6 and the content of calcium chloride in mortar (added to the mixing water) was 0, 0.5, 0.75, 1, 1.25, 1.5, 2, 3 and 4 % of cement weight. Dried sample of mortar (at 105°C) after 40 cycles of curing was crushed and ground in, so that no rest remained on the control sieve 0.200. The material was mixed with distilled water in the proportion 1: 4 by weight and it was leached for 6 hours at the temperature of (25 ± 5)°C. Every hour, the suspension was intensively shaken for 5 minutes and finally filtered. Subsequently the steel specimen, treated with sandpaper and degreased with acetone was immersed into the prepared mortar extract. Potentiodynamic measurement started after stabilization of steel potential.

Plotted dependences (current *i* vs. potential *E*) for calcium chloride content of 0%, 1.5% and 4% from Fig. 2 [8] were approximated by polynomials, from which the first and second order derivatives were determined. As could be seen in Fig. 4 distinct limits of *zero retardation* could be observed. In the region of passive state the *interval of zero retardation* is bordered by lower and upper limits of zero retardation. As expected, at the calcium chloride content of 0% it is more extensive comparing with the course belonging to content of 1.5%. At the content of 4% the upper and lower limits merge into one point, and the width of the interval is zero. The following limit of zero retardation is located in the transpassive region and represents additional important information about ongoing processes.

The obtained knowledge and experiences could be applied to a more detailed study of influences of accidental situations, e.g. exposition to fire [24], various types of overloadings [25, 26], degradation effects at the failure of a nuclear power plant, leakage and diffusion of aggressive media [27, 28, 29] and carbonation [30] as factors influencing the steel reinforcement corrosion in a given environment.

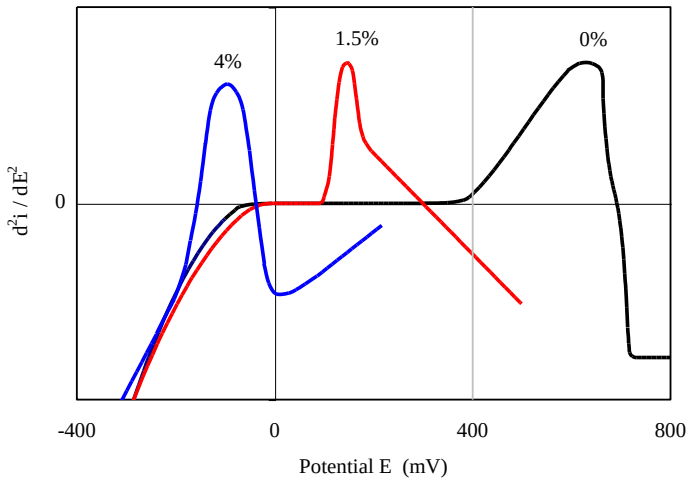

Fig. 4: Second order derivative of potentiodynamic curves of steel reinforcement in extracts of mortar samples at the polarization rate 30 mV.min^{-1} (40 cycles). Content of calcium chloride in mortar 0%, 1.5% and 4% of cement by weight.

4. Conclusions

The first and the second order derivatives of potentiodynamic diagrams represent very sensitive tools for the detection of ongoing processes at the investigation of corrosion of steel reinforcement in concrete.

Especially the limits of zero retardation and intervals of zero retardation seem to be very suitable for practical diagnostic.

The expression of presented diagram characteristics by physical parameters allows more concise assessment of effect of environment on corrosion behaviour of steel reinforcement.

More results, especially with regard to the variation of polarization rate, are necessary for creation of exact conclusions, applicable in the practice.

Acknowledgement

The work was supported by grants No. 2/0082/14 and No. 2/0033/15 of the Slovak Grant Agency (VEGA) as well as by grant APVV-0179-10.

References

[1] THE HOLY BIBLE, Genesis 13:12.

[2] SLUIJTER, W.L. – KREIJGER, P.C.: Potentio dynamic polarization curves and steel corrosion. Heron, Vol. 22 (1977), No. 1, pp. 13-27.

[3] ACI 222R-01 Protection of metals in concrete against corrosion. ACI Committee 222, 2001, 41 pp.

[4] STN 73 1341 Corrosion protection of reinforcements provided by the properties of concrete. Methods of test. SÚTN Bratislava, 1987, 20 pp.

[5] KINNUNEN, P.: Electrochemical characterisation and modelling of passive films on Ni- and Fe-based alloys. VTT Publications 472, Helsinki, 2002, 72 pp.

[6] HINDS, G.: The electrochemistry of corrosion. Edited by Gareth Hinds from the original work of J G N Thomas. National Physical Laboratory, Teddington, 2010, 25 pp.

[7] SAZOU, D. – PAVLIDOU, M. – DIAMANTOPOULOU, A. – PAGITSAS, M.: Oscillatory phenomena as a probe to study pitting corrosion of iron in halide-containing sulfuric acid solutions. Pitting corrosion. Chapter 4. InTech, 2012, 178 pp., ISBN 978-953-51-0275-5.

[8] KRAJČI, Ľ.: Diagnostic of reinforcement condition of reinforced concrete structures by electrical methods and the assessment of their reliability. Doctoral thesis, Slovak Academy of Sciences, Bratislava, 1999.

[9] NOSEK, V.: Electrochemical corrosion. Lecture No. 2. Technical University Liberec, Faculty of Mechanical Engineering, Department of Materials. Liberec, 2012, 39 pp.

[10] DAO, L.T.N. – DAO, V.T.N. – KIM, S-H. – ANN, K.Y.: Modeling steel corrosion in concrete structures – Part 1: A new inverse relation between current density and potential for the cathodic reaction. International Journal of Electrochemical Science, Vol. 5 (2010), pp. 302-313.

[11] KIM, CH-Y – KIM, J-K.: Numerical analysis of localized steel corrosion in concrete. Construction and Building Materials, Vol. 22 (2008), pp. 1129-1136.

[12] KEAR, G. – WALSH, F.C.: The characteristics of a true Tafel slope. Corrosion & Materials, Vol. 30 (2005), No. 6, pp. 1-4.

[13] LORBEER, P. – LORENZ, W.J.: A critical consideration of the Flade potential. Corrosion Science, Vol. 21 (1981), pp. 79-86.

[14] GERISCHER, H.: Remarks on the electronic structure of the oxide film on passive iron and the consequences for its electrode behaviour. Corrosion Science, Vol. 29 (1989), pp. 191-195.

[15] CAHAN, B.D. – CHEN, CH.T.: The nature of the passive film on iron: II . AC impedance studies. Journal of the Electrochemical Society, Vol. 129 (1982), No. 3, pp. 474-480.

[16] VERWEY, E.J.W.: Electrolytic conduction of a solid insulator at high fields. The formation of the anodic oxide film on aluminium. Physica, Vol. 2 (1935), pp. 1059-1063.

[17] CABRERA, N. – MOTT, N.F.: Theory of the oxidation of metals. Reports on Progress in Physics, Vol. 12 (1949), No. 1, pp. 163-184.

[18] KIRCHHEIM, R. – HEINE, B. – HOFMANN, S. – HOFSÄSS, H.: Compositional changes of passive films due to different transport rates and preferential dissolution. Corrosion Science, Vol. 31 (1990), pp. 573-578.

[19] CASTRO, E.B.: Analysis of the impedance response of passive iron. Electrochimica Acta, Vol. 39 (1994), pp. 2117-2123.

[20] MACDONALD, D.D. – SMEDLEY, S.I.: An electrochemical impedance analysis of passive films on Nickel (111) in phosphate buffer solutions. Electrochimica Acta, Vol. 35 (1990), pp. 1949-1956.

[21] BEVERSKOG, B. – BOJINOV, M. – ENGLUND, A. – KINNUNEN, P. – LAITINEN, T. – MÄKELÄ, K. – SAARIO, T. – SIRKIÄ, P.: A mixed-conduction model for oxide films on Fe, Cr and Fe-Cr alloys in high-temperature aqueous electrolytes. I. Comparison of the electrochemical behaviour at room temperature and at 200 °C. Corrosion Science, Vol. 44 (2002), No. 9, pp. 1901-1921.

[22] BOJINOV, M. – FABRICIUS, G. – KINNUNEN, P. – LAITINEN, T. – MÄKELÄ, K. – SAARIO, T. – SUNDHOLM, G.: The mechanism of transpassive dissolution of Ni-Cr alloys in sulphate solutions. Electrochimica Acta, Vol. 45 (2000), pp. 2791-2802.

[23] BOJINOV, M. – FABRICIUS, G. – KINNUNEN, P. – LAITINEN, T. – MÄKELÄ, K. – SAARIO, T. – SUNDHOLM, G. – YLINIEMI, K.: Transpassive dissolution of Ni-Cr alloys in sulphate solutions – comparison between a model alloy and two industrial alloys. Electrochimica Acta, Vol. 47 (2002), pp. 1697-1712.

[24] JANOTKA, I. – MOJUMDAR, S.C.: Thermal analysis at the evaluation of concrete damage by high temperatures. Journal of Thermal Analysis and Calorimetry, Vol. 81 (2005), No. 1, pp. 197-203.

[25] MELCER, J. – LAJČÁKOVÁ, G.: Severe load test of a bridge and its consequences. Proceedings of the International Conference on Reliability of Structures. Ostrava, 2003, pp. 93-96.

[26] TESAR, A.: The ultimate response of slender bridges subjected to braking forces. Proceedings of the First International Conference on Railway Technology: Research, Development and Maintenance, Las Palmas de Gran Canaria, Spain. Paper 4. Civil-Comp Press, 2012, pp. 1-13.

[27] JANOTKA, I. – KRAJČI, Ľ.: Effect of polymer on structural characteristics and steel corrosion of cement-poor mortar. Chemical Papers, Vol. 58 (2004), No. 2, pp. 79 – 86.

[28] JERGA, J. – HALAS, P.: Ingress of chloride into the prestressed concrete structure. Proceedings of the 5th International Conference on Concrete. Prague: ICC; 1990, pp. 400–404.

[29] KRAJČI, Ľ.: Relation of cement matrix deterioration to steel reinforcement corrosion of mortars in aggressive environment. Building Research Journal, Vol. 54 (2006), No. 3-4, pp. 233-241.

[30] KRAJČI, Ľ. – JANOTKA, I.: Measurement techniques for rapid assessment of carbonation in concrete. ACI Materials Journal Vol. 97 (2000), pp. 168-171.